FEBS Letters 588 (2014) 1755–1766

FEBS Letters

journal homepage: www.FEBSLetters.org

Characterization of residue-dependent differences in the peripheral membrane association of the FATC domain of the kinase 'target of rapamycin' by NMR and CD spectroscopy

Lisa A.M. Sommer [a], Sonja A. Dames [a,b,*]

[a] Chair of Biomolecular NMR Spectroscopy, Department of Chemistry, Technische Universität München, Lichtenbergstr. 4, 85747 Garching, Germany
[b] Institute of Structural Biology, Helmholtz Zentrum München, Ingolstädter Landstr. 1, 85764 Neuherberg, Germany

ARTICLE INFO

Article history:
Received 30 January 2014
Revised 14 March 2014
Accepted 17 March 2014
Available online 3 April 2014

Edited by Sandro Sonnino

Keywords:
Target of rapamycin
Kinase
Protein lipid interaction
Protein membrane interaction
Membrane mimetic
Micelle
Bicelle
Liposome
Small unilamellar vesicles
NMR
CD

ABSTRACT

The conserved C-terminal FATC domain of the kinase 'target of rapamycin' is important for its regulation and was suggested to contain a peripheral membrane anchor. Here, we present the characterization of the interactions of the yeast TOR1 FATC domain (2438–2470 = y1fatc) and 15 mutants with membrane mimetic micelles, bicelles, and small unilamellar vesicles (SUVs) by NMR and CD spectroscopy. Replacement of up to 6–7 residues did not result in a significant abrogation of the association with micelles or bicelles. However, replacement of only one residue could result in an impairment of the interaction with SUVs that are usually used at low concentrations. Some mutants not binding liposomes may be introduced in full-length TOR for future functional and localization studies *in vivo*.

1. Introduction

The conserved multidomain serine/threonine kinase mammalian/mechanistic target of rapamycin (mTOR) integrates different cellular signals in response to nutrients and growth factors to centrally regulate growth, metabolism and longevity [1,2]. Impairment of TOR function is involved in the development of different metabolic, cardiovascular, and neurodegenerative diseases [1–4].

The TOR signaling network consists of two major branches, each mediated by a specific complex with other proteins. TOR complex1 (TORC1) is very sensitive to the TOR-specific inhibitor complex rapamycin-FKBP12 (FK506-binding protein of 12 kDa) and regulates processes such as protein and lipid synthesis, ribosome biogenesis, autophagy, glycolysis, and angiogenesis [5,6]. TOR complex2 (TORC2) is rather insensitive to rapamycin and is involved in the control of cytosceletal organization, gluconeogenesis, and cell survival [5–7].

TOR proteins contain different functional regions (Fig. 1A). The N-terminal HEAT repeat region (~1200 residues) and the following FRAP ATM TRRAP (FAT) domain (~550 residues) are composed of α-helical repeat motifs (HEAT, tetratricopeptide (TRP) repeats) that typically form platforms mediating protein–protein interactions [8–10]. The FKBP12–rapamycin-binding (FRB, ~100 residues) domain forms a four-α-helix bundle and contains the binding site for the TOR-specific inhibitor complex composed of the cellular protein FKBP12 and the macrolide rapamycin [11]. C-terminal of the catalytic kinase domain (~250–350 residues) is the highly

Abbreviations: CMC, critical micelle concentration; DihepPC, 1,2-diheptanoyl-*sn*-glycero-3-phosphocholine; DMPC, 1,2-dimyristoyl-*sn*-glycero-3-phosphocholine; DPC, dodecylphosphocholine; FAT(C), FRAP, ATM, TRRAP (C-terminal); GB1, B1 immunoglobulin binding domain of streptococcal protein G (56 residues); gb1xa, GB1 followed by a thrombin and a factor Xa recognition site (=GB1-LVPRGS-IEGR); PIKK, phosphoinositide-3 kinase-related kinase; (m)TOR, (mammalian/mechanistic) target or rapamycin; min, minute(s); SI, supplementary information; y1fatc, residues 2438-2470 of *S. cerevisiae* TOR1

* Corresponding author at: Chair of Biomolecular NMR Spectroscopy, Department of Chemistry, Technische Universität München, Lichtenbergstr. 4, 85747 Garching, Germany. Fax: +49 89 28913869.

http://dx.doi.org/10.1016/j.febslet.2014.03.031
0014-5793/

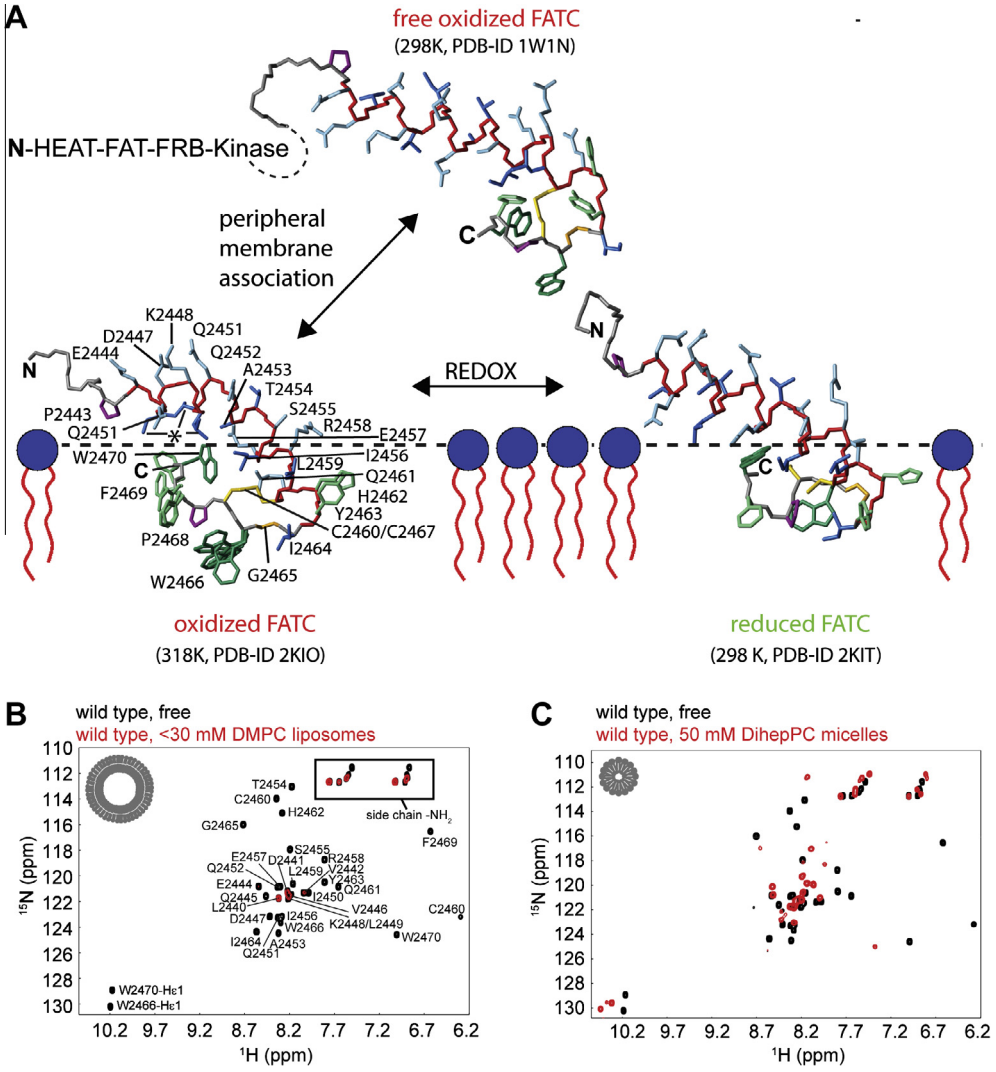

Fig. 1. Summary of the current structural data for the yeast TOR1 FATC domain (=y1fatc) and the current model for membrane association and NMR-monitored interaction studies with neutral liposomes and diacyllipid micelles. (A) The top representation shows the structure of the free oxidized form [18]. As indicated, the FATC domain is at the C-terminus of TOR and is in the full-length protein preceded by the kinase, the FRB, and the FAT domains. The N-terminal region is composed of HEAT repeats. The bottom panel shows the structures of the micelle immersed oxidized and reduced y1fatc protein [23]. The model for membrane immersion has been derived based on the interaction surface derived from a titration with DPC and the surface charge distribution and was modified from [23]. The membrane-solvent interface is indicated by a black dotted line. The membrane lipids are schematically sketched by a blue circle for the headgroup and red, wavy lines for the acylchains. The backbone of the α-helix is depicted in red. The side chains of aromatic residues (W, Y, F, H) are colored green, those of residues with methyl groups in the side chain (L, I, V, T, A) darker blue, and those of residues with polar or charged side chains light blue. The conserved glycine is depicted in orange and the side chains of the disulfide bond forming cysteines in yellow. The structure of oxidized micelle immersed y1fatc had to be determined at 318 K, because at lower temperatures the NMR signals for the micelle immersed region are partially not visible [23]. For oxidized micelle immersed y1fatc, the side chains of W2466 and F2469 are shown for several structures of the calculated ensemble to indicate the greater structural heterogeneity around these residues. The residues are labeled with the one-letter amino acid code and the sequence position in full-length yeast TOR1 (*: V2448, L2449, I2450). (B) and (C) Superposition of the ^{1}H-^{15}N-HSQC spectra of oxidized wild type y1fatc in the absence and presence of DMPC SUVs and DihepPC micelles, respectively. The color coding is indicated at the top of each plot. Both plots show in grey simple schematic representations of the respective membrane mimetic particles.

conserved FATC domain (well conserved region ~33 residues, see SI Fig. S1A). This domain has been shown to play a very important role for the regulation of TOR and the other phosphoinositide-3 kinase-related kinase (PIKK) family members [8,12–17].

Fig. 1A provides a summary of the current structural data for the FATC domain of yeast TOR1 (residues 2438–2470 = y1fatc). The structure of the free oxidized form consists of an α-helix that is followed by a disulfide bonded loop (PDB-ID 1w1n). Reduction of the disulfide bond formed between the highly conserved cysteines C2460 and C2467 increases the flexibility of the C-terminal half, which may modulate the interactions with TOR regulators [18]. Based on a fluorescence assay the redox-potential of this disulfide bond is −0.23 V and thus in a range allowing the redox state to be modulated by typical cellular redox regulators. Additional *in vivo* mutagenesis studies in yeast showed that replacement of one of the disulfide forming cysteines lowers the cellular stability of TOR [18]. Consistent with this, a redox-sensitive formation of TORC1 and its signaling function was suggested [19–22]. Analysis of the FATC sequence with the program e-motif (G. Tevzadze personal communication) suggested that the C-terminal end that is rich in aromatic residues (Fig. 1A, SI Fig. S1A) might contain a lipid binding motif. NMR-monitored binding studies with different lipids and membrane mimetics showed that the TOR FATC domain only interacts with lipids above the critical micelle concentration (CMC), however does not show a very pronounced preference for specific headgroups or membrane properties such as surface charge and shape or the packing density of the lipid acyl chains [23]. Both redox states of y1fatc can interact with

membrane mimetics. The bottom panel of Fig. 1A shows the three-dimensional structures of the micelle immersed oxidized and reduced forms (PDB-ID 2kio and 2kit) [23]. The association with micelles maintains the overall fold of the oxidized state, however the α-helix is stabilized and extends more to the C-terminus. Although not restricted by a disulfide bond, the C-terminus of the reduced micelle immersed state also folds back to the α-helix. The orientation of side chains in the C-terminal micelle immersed loop is however slightly different between the oxidized and the reduced form. Based on an estimate of the Kd from NMR diffusion data, the oxidized form has a slightly higher affinity for DPC micelles than the reduced one [23]. In both micelle immersed states the α-helix is slightly kinked and distorted around A2453, which is presumably near the interface between the micelle and the solvent. The initial model of the membrane immersion of the oxidized and reduced TOR FATC domain shown in Fig. 1A was derived based on the micelle-binding surface derived from the titration of oxidized y1fatc with DPC and the surface charge distribution [23]. Based on this model the hydrophobic residues in the C-terminal bulb-like region (I2456-W2470 in y1fatc) may penetrate the micelle and interact with the hydrophobic acyl chains, whereas a rim of charged residues (E2457, R2458, C-terminal carboxyl group in y1fatc) may interact with charges in the lipid headgroups [23]. Based on recent NMR- and CD-monitored binding studies, the FATC domains of the other human PIKK family members including ataxia-telangiectasia mutated (ATM), ataxia- and Rad3-related (ATR), DNA-dependent protein kinase catalytic subunit (DNA-PKcs), suppressor of morphogenesis in genitalia (SMG-1), and transformation/transcription domain-associated protein (TRRAP) can also interact with membrane mimetics, which results generally in an increase of the α-helical secondary structure content [24].

TOR has been localized at various cellular membranes such as the plasma membrane and the outer membranes of the ER, Golgi, mitochondria, lysosomes, and peroxisomes [22,25–31]. In addition it was found in the nucleus and associated with ribosomes [32,33]. Direct membrane interactions of TOR may be mediated by the FRB domain and as described above by the C-terminal FATC domain [23,34,35]. Overall, the localization appears to depend on the exact composition of the TOR complexes as well as on the cell type and signaling state. Recently it has been highlighted that membrane clustering influences the signal response and that spatial portioning improves the reliability of biochemical signaling [36,37]. Thus the specific signaling output of TOR may depend on its localization [22], which likely is regulated by a network of protein–lipid/–membrane and protein–protein interactions.

In order to better understand the importance of different mostly conserved hydrophobic residues and a glycine in the y1fatc membrane anchor for the interaction with different membranes, we analyzed the interactions of wild type y1fatc and a large array of mutants (Table 1) with different membrane mimetics (SI Fig. S1B) by NMR and CD spectroscopy. Based on the presented data the choice of the membrane mimetic and the concentration at which it is used are important factors to detect small binding differences between the wild type and mutant forms. Since some of the mutated residues are also conserved in the FATC domains of other PIKKs, the results are not only interesting to design full-length mutants for TOR but also for the other PIKKs for *in vivo* functional and localization studies.

2. Materials and methods

2.1. Mutagenesis and protein expression and purification

The wild type FATC domain of yeast TOR1 (residues 2438–2470 = y1fatc) was prepared as described earlier [18] and below.

Table 1
Summary of the NMR-monitored membrane mimetic binding studies of wild type and mutant y1fatc.

y1fatc protein*	gb1xa tag	Micelles	Bicelles	SUVs
Wild type	Yes & no	+	+	+
L2459A	Yes & no	+	+	+
H2462A	no	+	n.d.	n.d.
Y2463A	Yes & no	+	+	–
F2469A	No	+	n.d.	n.d.
W2466A	No	+	n.d.	–
W2466A/W2470A	No	+	n.d.	–
Y2463A/I2464A/W2466A/W2470A	No	+	n.d.	n.d.
Y2463E/W2466E	Yes & no	+	+	–
Y2463D/I2464D/W2466A	Yes	+	+	–
Y2463D/I2464D/W2466E/W2470R	Yes	+	+	–
H2462R/Y2463D/I2464D/W2466A/F2469D	Yes	+	+	–
G2465S/W2466S	Yes	+	+	–
H2462R/Y2463D/I2464D/G2465S/W2466S/F2469D	Yes	+	+	–
L2459E/H2462R/Y2463D/I2464D/G2465S/W2466A/F2469D	Yes	+	n.d.	–
L2459S/H2462R/Y2463D/I2464D/W2466E/F2469D	Yes	+	n.d.	–

+ = Strong spectral changes indicating an interaction with the respective membrane mimetic, – = no significant spectral changes/interaction, n.d. = not determined.
* Regarding the interaction of the W2466A and W2466A/W2470 mutants with DPC see [23].

Replacement of one or more residues by alanine or other amino acids was achieved by mutagenesis following the QuickChange site directed mutagenesis protocol (Stratagene). Table 1 shows an overview of all prepared mutated FATC proteins. All proteins were overexpressed in *Escherichia coli* BL21 (DE3) in LB or ^{15}N-M9 minimal medium. The culture was grown until an OD_{600} of ~0.7–0.9, following induction with 1 mM IPTG for 3 h at 37 °C. The fusion protein consisting of the B1 domain of protein G (GB1), a thrombin (LVPRGS) and a factor Xa (IEGR) site as well as y1fatc, as wild type or mutated variant, (=y1fatc-gb1xa, 99 residues in total), was mainly expressed soluble. If needed, the inclusion body fraction was extracted as described [18]. The purification of the fusion proteins followed either the original protocol using ultrasonication for cell lysis [18] or a heat shock protocol [38]. The lysis buffer was always 50 mM Tris, 2 mM benzamidine, 2 mM EDTA, pH 7.5. GB1 fusion protein in the supernatant after cell lysis was extracted by IgG affinity chromatography as described in the manufacturer's manual (GE Healthcare). The purified protein was lyophilized and resuspended in 50 mM Tris, 100 mM NaCl, pH 6.5 (NMR buffer). If the GB1 fusion protein was directly used for NMR-monitored binding studies as suggested recently [39], the resuspended protein was concentrated and washed several times with NMR buffer using ultrafiltration spin columns (Amicon Ultra, Merck Millipore, MWCO 3000).

To obtain pure y1fatc, wild type or mutated, the IgG Sepharose purified fusion protein resuspended in 50 mM Tris, 100 mM NaCl, pH 8.0 containing additionally 2 mM $CaCl_2$ was digested overnight with factor Xa. The cleaved off fusion tag was subsequently removed by RP-HPLC using a C4 column and an acetonitrile/trifluoroacetic acid buffer system and fractions containing pure y1fatc or the mutated version were lyophilized and resuspended in 50 mM Tris, 100 mM NaCl, pH 6.5 as described [18]. The correct molecular weight of the used proteins was confirmed by mass spectrometry.

2.2. Sample preparation for NMR experiments

Dodecylphosphocholine (DPC) and 1,2-dimyristoyl-sn-glycero-3-phosphocholine (DMPC) were purchased from Avanti Polar Lipids. In addition, 1,2-Diheptanoyl-*sn*-glycero-3-phosphocholine (DihepPC) and DMPC were obtained from Affymetrix. Deuterated d_{38}-DPC was bought from Cambridge Isotope Laboratories. For the titrations with different lipids or lipid mixtures, the protein concentration was in the range of 20–200 μM in 50 mM Tris, 100 mM NaCl, 0.02% NaN_3 (95% H_2O/5% D_2O), pH 6.5. Lipid stock solutions for the titrations or samples with a defined lipid concentration were prepared as follows. A defined amount of lipid from a concentrated stock in chloroform was placed in a glass vial and dried under a stream of nitrogen gas. The dried lipid was then dissolved in buffer or the protein sample and the pH adjusted to 6.5. For the samples with DMPC/DihepPC bicelles (q = 0.2, [DMPC] = 0.032–0.04 M, [DihepPC] = 0.16–0.20 M corresponding to c_L = 12–15%) the appropriate amount of a DMPC stock solution in chloroform was placed in a glass vial and dried under a stream of nitrogen gas. Bicelles were formed by stepwise addition of the appropriate amount of a DihepPC stock solution in buffer and vigorous vortexing after each step. Lastly, the protein solution was added and everything mixed by vortexing.

For the preparation of liposomes, an appropriate amount of DMPC in chloroform needed for a 50 mM solution was placed in a glass vial and dried under a stream of nitrogen gas. The lipid was resuspended in buffer and dissolved by seven cycles of freezing in liquid nitrogen, incubation in a water bath at 40 °C, and vigorous vortexing. The formation of small unilamellar vesicles (SUVs) was induced by incubation in an ultrasonic bath for about half an hour (T kept < ~30–35 °C). After centrifugation for 5 min at maximum speed in a table top centrifuge the clear supernatant of the suspension was used for the NMR samples (using the 50 mM stock solution the final sample contained <30 mM DMPC). The fluffy white precipitate containing large uni- and multilamellar vesicles was discarded.

2.3. Sample preparation for CD experiments

The protein concentration for CD experiments of wild type and mutant y1fatc proteins was about 30 μM in 50 mM Tris, 100 mM NaCl, pH 6.5. The samples in the presence of micelles, bicelles, or liposomes were prepared as described for the NMR samples.

2.4. NMR spectroscopy

NMR spectra were acquired at 298 and 318 K on Bruker Avance 500 and 750 MHz spectrometers, the 500 MHz one equipped with a cryogenic probe. The data were processed with NMRPipe [40] and analyzed using NMRView [41].

2.5. CD spectrometry

CD spectra were recorded on a Jasco J-715 spectropolarimeter at 25 °C in the range of 190–260 nm using a quartz cuvette with a path length of 0.1 cm. All spectra were recorded with an acquisition time of 50 nm per minute and 5 scans. The response time was 8 s.

3. Results

3.1. The TOR FATC domain interacted with DMPC liposomes and DihepPC micelles

Recently we have shown that yeast TOR1 FATC domain (residues 2438–2470 = y1fatc, Fig. 1A, SI Fig. 1A) can interact with neutral DPC micelles (Fig. 2A), negatively charged membrane mimetic particles prepared from dioctanoyl-phosphatidic acid (PA), a 4:1 mixture of dioctanoyl- and dioleoyl-PA, or dihexanoyl-phospho-inositol-3,4,5-trisphosphate and DPC, and with neutral DihepPC/DMPC bicelles (Fig. 3A) and determined the structures of oxidized and reduced y1fatc immersed in DPC micelles [23].

Since liposomes are considered a more realistic mimetic for natural membranes than micelles or bicelles, we first analyzed if y1fatc can also interact with neutral DMPC small unilamellar vesicles (SUVs, SI Fig. S1B). In the presence of liposomes at a DMPC concentration below 30 mM (Fig. 1B) several peaks of y1fatc disappeared in the respective ^1H-^{15}N-HSQC spectra. This indicated that y1fatc interacted with the large DMPC SUVs, resulting in a broadening of most of its NMR signals beyond detection.

Although DPC has as DMPC a neutral phosphocholine headgroup, it resembles with its single fatty acid chain more a lysolipid (SI Fig. S1B). In previous studies the interaction with micelles composed of a lipid with two acyl chains has only been analyzed using negatively charged dioctanoyl-PA. The resulting spectral changes were overall similar as with DPC [23]. For completion and because DihepPC is used as rim component in the below described interaction studies with bicelles, we characterized also the interaction with micelles composed of the neutral diacyllipid DihepPC (SI Fig. 1B). The overall NMR spectral changes in the presence of DihepPC micelles (Fig. 1C) were similar as with DPC micelles (Fig. 2A) and DMPC/DihepPC bicelles (Fig. 3A). Based on the presented and earlier data [23], the wild type FATC domain of TOR binds to membrane mimetics as diverse as micelles, bicelles, and liposomes and to membrane mimetics composed of only neutral components or containing additionally negatively charged lipids such as phosphatidic acid (PA), or phosphatidylinositol lipids (PIPs). In combination, these data confirm that the wild type TOR FATC domain does not show strong specific preferences for membrane properties such as the presence of specifically shaped headgroups or the surface charge and curvature or the packing properties of the lipid acyl chain.

3.2. Mutation of up to 7 residues in the y1fatc membrane anchor did not abrogate the interaction with DPC micelles

Tryptophans are known to play an important role for the membrane interactions of proteins and short tryptophan-rich peptides can interact with membrane mimetics [42,43]. Because of this, the effect of replacing one or both tryptophans by alanine (y1fatc W2466A and W2466/W2470A) on the interaction with DPC micelles has been analyzed in initial mutagenesis studies. However, neither mutant showed a strongly reduced affinity for DPC micelles [23]. This suggested that the other aromatic and aliphatic residues in the y1fatc membrane anchor (Fig. 1A) contribute significantly to the binding affinity. To better understand the role of the other hydrophobic residues and of the conserved glycine for the interaction with membrane mimetics and to find a mutant that no longer interacts with membrane mimetics for future *in vivo* functional and localization studies, we analyzed the interactions of 13 additional y1fatc mutants (Table 1) with DPC micelles, DihepPC/DMPC bicelles and DMPC liposomes of the SUV type by NMR and CD spectroscopy (Figs. 2–5, SI Figs. S2–S6).

DPC micelles are a well characterized membrane mimetic often used for the structural characterization of membrane interacting proteins [44–46]. Therefore, we first probed the effect of mutations on the binding affinity by comparing for each mutant the ^1H-^{15}N-HSQC spectra in the absence and presence of DPC micelles (Fig. 2, SI Fig. S2/S3). First, additional y1fatc single mutant proteins were prepared by replacing one hydrophobic residue at a time in the membrane anchor by alanine (L2459A, H2462A, Y2463A, and F2469A, Table 1). Fig. 2B shows representatively the superpositions

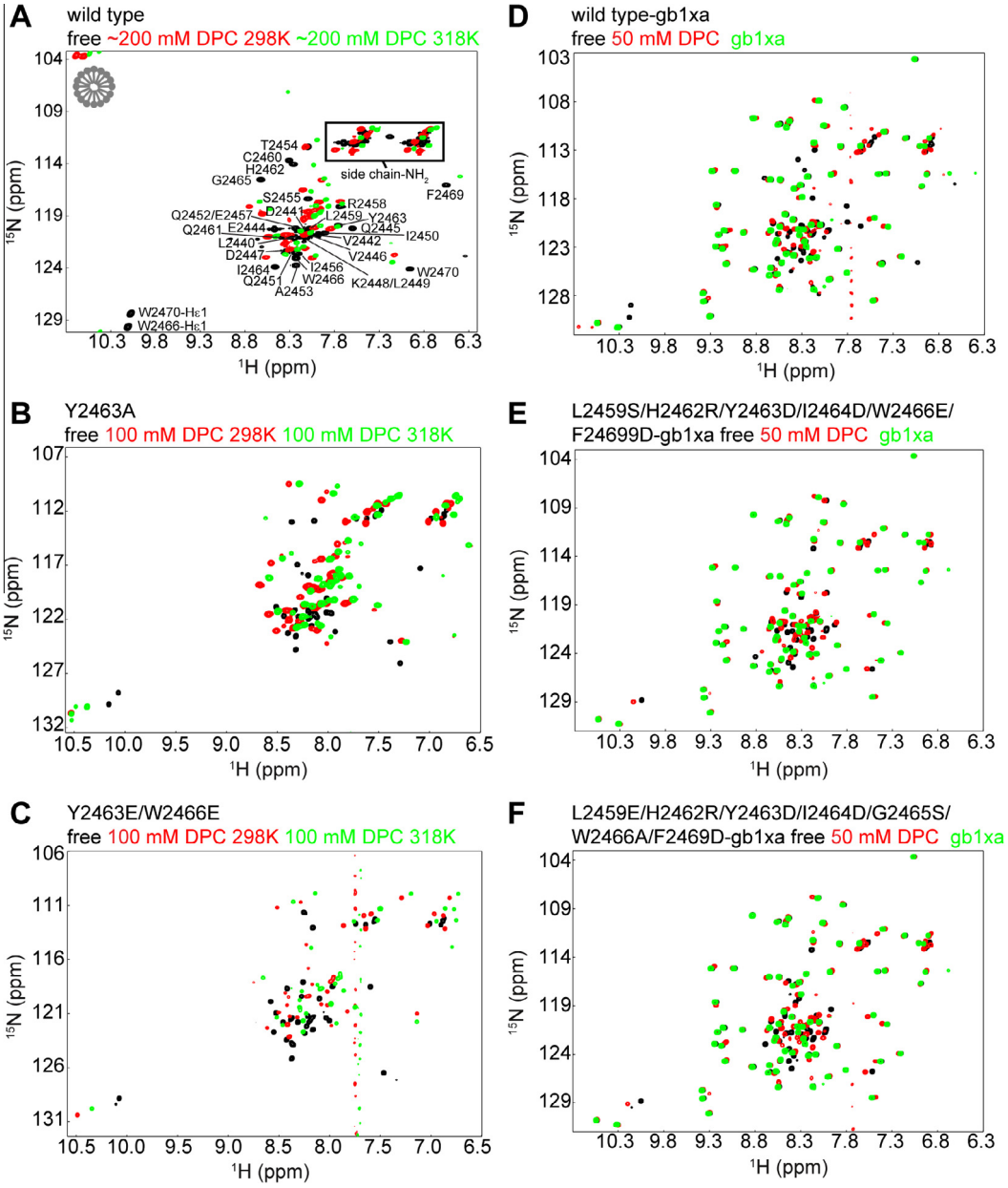

Fig. 2. NMR characterization of the interaction of the untagged and GB1-tagged yeast TOR1 FATC domain and selected mutants with membrane mimetic DPC micelles. (A–C) Superposition of the ^{1}H-^{15}N-HSQC spectra of untagged y1fatc (A, adapted from [23]) and the Y2463A and Y2463E/W2466E mutants (B–C) in the free state at 298 K and in the presence of DPC micelles at 298 K and 318 K. Increasing the temperature lowers the interaction with DPC micelles thereby enabling also the detection of signals corresponding to the central region of the membrane anchor (e.g. green peak ~108 ppm corresponding to G2465 in the bound state) [23]. The assignments for free y1fatc are indicated with the one-letter amino acid code and the sequence position in full-length yeast TOR1 [18]. (D–F) Superposition of the ^{1}H-^{15}N-HSQC spectra of GB1-tagged wild type y1fatc and the indicated mutants with 6 or 7 replacements in the absence and presence of DPC micelles. For all the spectrum of the GB1 tag alone that is followed by a factor Xa site (=gb1xa) is shown on top in green to better differentiate the peaks of the FATC part and the tag. As shown earlier the GB1tag does not interact with membrane mimetic micelles, bicelles, or SUVs [39]. Accordingly the respective peaks do not significantly shift upon addition of the respective membrane mimetic. The color coding of all NMR spectra and the used DPC concentrations are indicated at the top of each plot. (A) Shows in grey a simple schematic representation of the respective membrane mimetic particle.

of the ^{1}H-^{15}N-HSQC spectra of the Y2463A mutant in the absence (black) and presence (red) of a high concentration of DPC micelles (100 mM DPC). The data for the L2459A, H2462A, and F2469A mutants are given in Supplementary Fig. S2B–D. As the wild type (Fig. 2A) and the W2466A mutant [23], all newly prepared single mutants showed strong spectral changes and a spectrum different from the free form with well-dispersed peaks. Thus all could still interact with DPC micelles. Oxidized micelle immersed wild type y1fatc at 298 K shows fewer peaks than expected based on the number of residues in the sequence, because several of the peaks of the membrane anchor are not visible [23]. They become only visible if the temperature is raised to 318 K, which reduces the affinity of the interaction with micelles (Fig. 2A green spectrum and [23]). Based on a comparison of the number of peaks visible for the respective micelle immersed y1fatc mutants at 298 and 318 K with the respective wild type data (Fig. 2A–B, SI Fig. S2), single replacements by alanine had no strong effect on the affinity. All showed, like the wild type, an increase of the number of peaks at 318 K, which appeared only somewhat less for the mutant Y2463A (Fig. 2B). However, some single mutants showed a greater

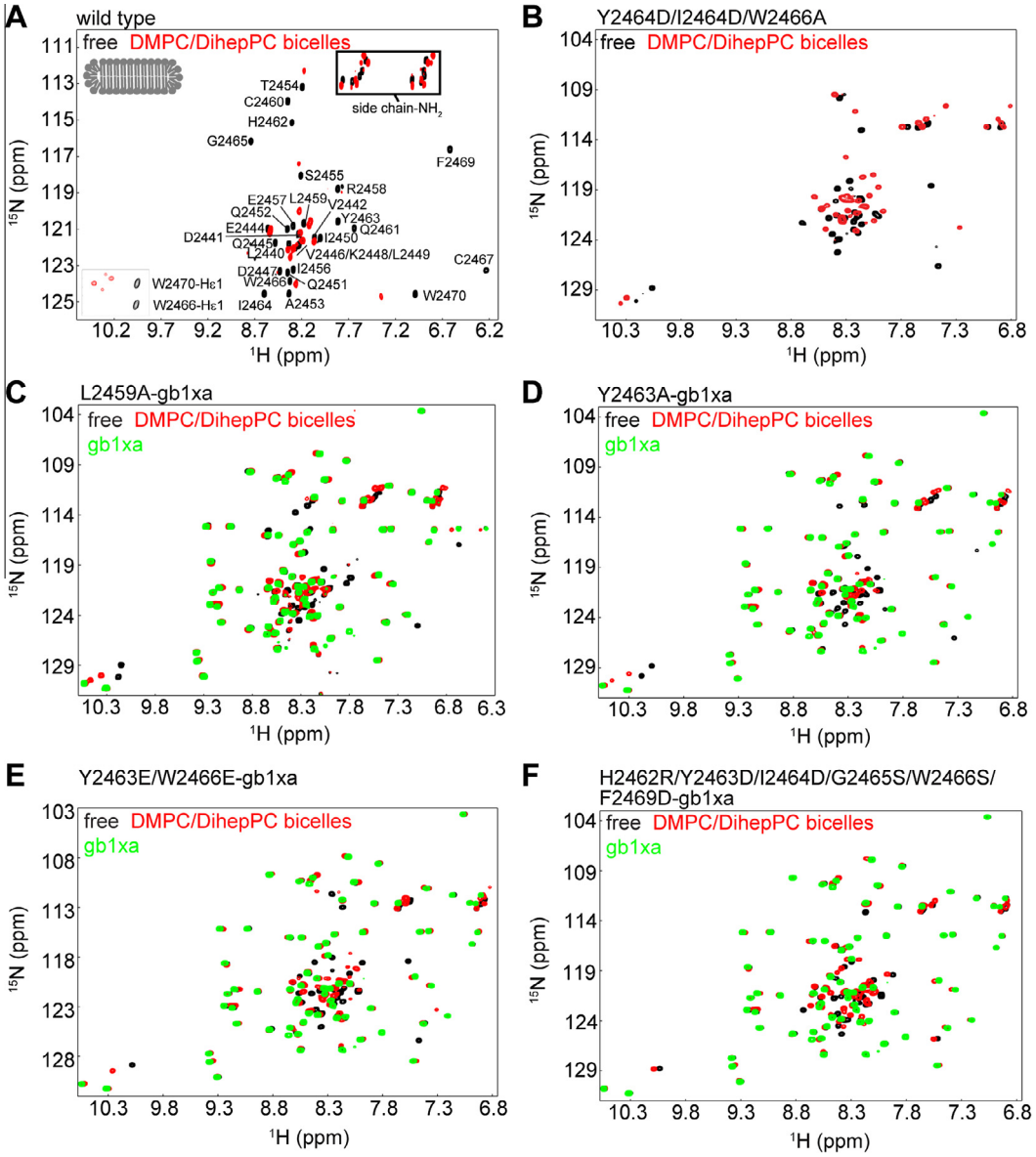

Fig. 3. NMR characterization of the interaction of the untagged and GB1-tagged yeast TOR1 FATC domain and selected mutants with membrane mimetic DMPC/DihepPC bicelles (q 0.2, c_L 12–15%). (A–B) Superposition of the ^{1}H-^{15}N-HSQC spectra of untagged oxidized y1fatc (A, adapted from [23]) and the Y2463D/I2464D/W2466A mutant (B) in the absence and presence of bicelles. The insert in (A) shows the region for the tryptophan side chain amide groups that were spectrally folded due to a lower sweep width in the ^{15}N-dimension. The assignments for free y1fatc are indicated with the one-letter amino acid code and the sequence position in full-length yeast TOR1 [18]. (C–F) Superposition of the ^{1}H-^{15}N-HSQC spectra of the GB1-tagged y1fatc mutants L2459A, Y2463A, Y2463E/W2466E, and H2462R/Y2463D/I2464D/G2465S/W2466S/F2469D in the absence and presence of bicelles. For all the spectrum of the GB1 tag alone that is followed by a factor Xa site (=gb1xa) is shown on top in green to better differentiate the peaks of the FATC part and the tag. As shown earlier the GB1tag does not interact with membrane mimetic micelles, bicelles, or SUVs [39]. (A) shows in grey a simple schematic representation of the respective membrane mimetic particle.

conformational heterogeneity than the free and micelle immersed wild type protein. This was for example the case for the y1fatc mutants Y2463A (Fig. 2B) and H2462A (SI Fig. S2C). Several peaks appeared as some kind of doublet. For example, in the region ~10 ppm, where in case of a single conformation (or very fast dynamics), only one crosspeak should be visible for each side chain amide group of the two tryptophans. Thus H2462 and Y2463 may influence the backbone flexibility at the C-terminal end of the α-helix and in the disulfide bonded loop in the free and/or micelle immersed state. Alternatively or in addition, they may influence the rate of cis/trans isomerization of P2468 or alter the interactions within the C-terminal loop and with the surrounding micellar environment.

Since replacement of one or even two aliphatic or aromatic residues (for L2456A, H2462A, Y2463A, F2469A see Fig. 2B and SI Fig. S2B–D and for W2466A, W2466A/W2470A see [23]) by the less hydrophobic residue alanine did not significantly reduce the interaction with DPC micelles, additional mutants were prepared in which more hydrophobic residues were replaced by alanine or even polar or charged residues (Table 1). The quadruple y1fatc mutant Y2463A/I2464A/W2466A/W2470A showed, like the single or double alanine mutants, strong spectral changes in the presence of DPC micelles (SI Fig. S2E). This was similarly the case if two hydrophobic residues had been replaced by negatively charged amino acids as in the y1fatc mutants Y2463E/W2466E (Fig. 2C) or Y2463D/I2463D/W2466A (SI Fig. S2F). However, for all these

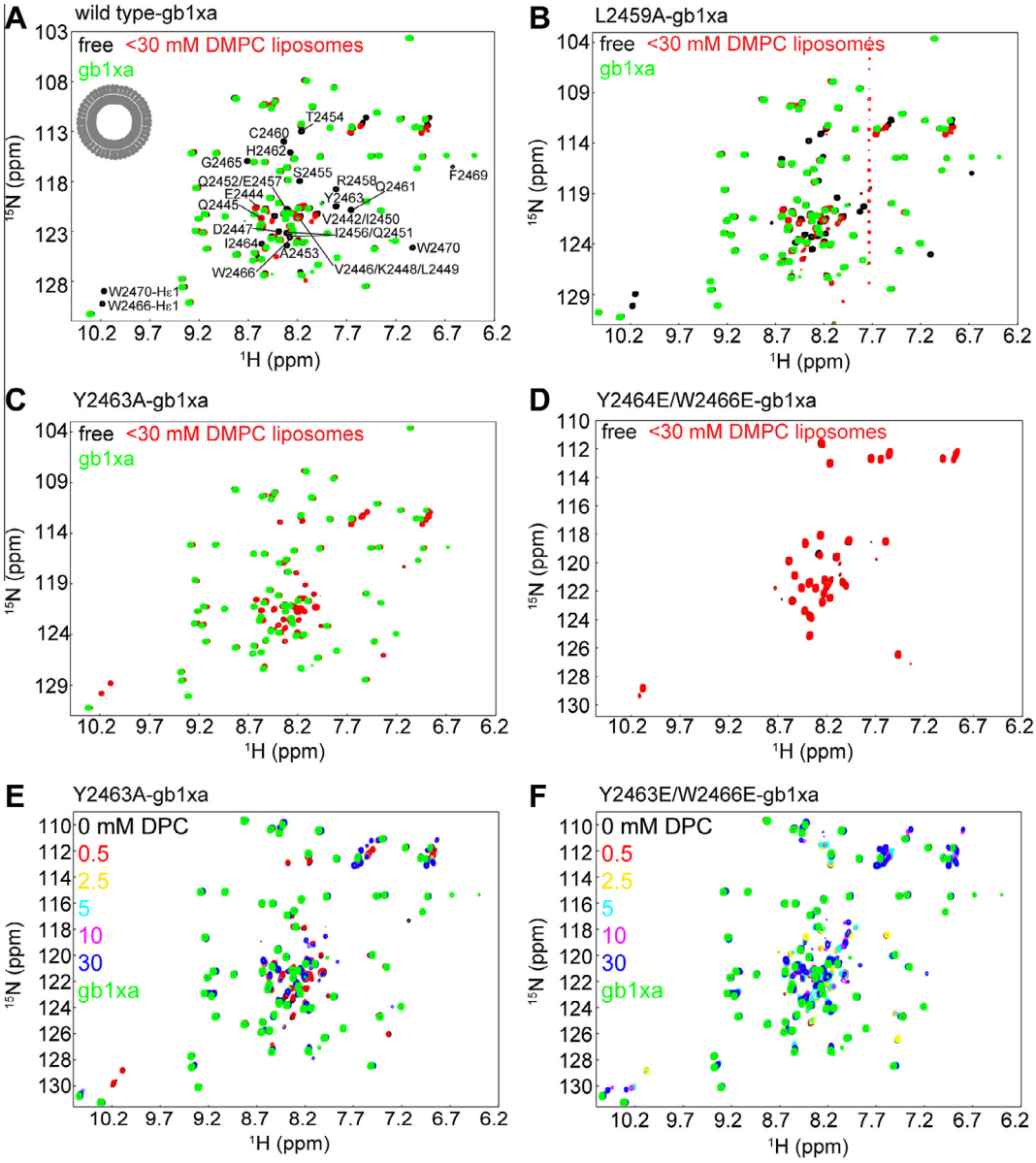

Fig. 4. NMR characterization of the interaction of GB1-tagged or untagged wild type and mutated yeast TOR1 FATC proteins with DMPC SUVs and low concentrations of DMPC. (A–D) Superposition of the ^{1}H-^{15}N-HSQC spectra of wild type GB1-tagged y1fatc (A, results for untagged see Fig. 1B) and the also GB1-tagged mutants L2459A and Y2463A as well as the untagged mutant Y2463E/W2466E in the absence and presence of DMPC SUVs. The assignments for free GB1-tagged y1fatc are, as far as they could be transferred from the untagged form, indicated with the one-letter amino acid code and the sequence position in full-length yeast TOR1 [18]. (E) and (F) Superposition of the ^{1}H-^{15}N-HSQC spectra of the GB1-tagged mutants Y2463E/W2466E and Y2463A in the absence and presence of increasing concentrations of DPC. The color coding of all NMR spectra is indicated in each plot. For the spectral superpositions of GB1-tagged proteins the spectrum of the GB1 tag alone that is followed by a factor Xa site (=gb1xa) is shown on top in green to better differentiate the peaks of the FATC part and the tag. As shown earlier the GB1tag does not interact with membrane mimetic micelles, bicelles, or SUVs [39]. (A) shows in grey a simple schematic representation of the respective membrane mimetic particle.

mutants the number and intensity of peaks of the micelle immersed form did not significantly increase at higher temperature, indicating a somewhat decreased affinity for DPC micelles compared to the wild type.

To find a mutation that abrogates the interaction with membrane mimetics, we designed additional mutants with more drastic replacements of hydrophobic residues by polar or charged ones. The preparation of the pure FATC domain is rather time-consuming and expensive. Recently, we showed that the GB1 fusion tag does not interact with membrane mimetic micelles, bicelles, or SUVs [39]. Consequently, NMR-monitored interaction studies of additional y1fatc mutant proteins could be done using directly the GB1-tagged protein. Because DPC has a small CMC (1.1 mM) and the GB1-tagged wild type y1fatc showed still strong spectral changes with 50 mM DPC (Fig. 2D), the interaction studies with GB1-tagged mutant proteins were also done at this DPC concentration. Surprisingly, replacement of up to 6 hydrophobic residues with mostly polar or charged residues (y1fatc-L2459S/H2462R/Y2463D/I2464D/W2466E/F2469D) still did not abrogate the interaction with DPC micelles that were used at a lower concentration as in the initial binding studies (Fig. 2E, SI Figs. S3A and B).

Thus, additional y1fatc mutants were prepared in which G2465 that was suggested to facilitate the formation of the disulfide bond was replaced by serine (y1fatc-G2465S/W2466S, -H2462R/Y2463D/I2464D/G2465S/W2466S/F2469D, and -L2459E/H2462R/Y2463D/I2464D/G2465S/W2466A/F246D). The hypothesis was that this mutant may not as easily form the C-terminal bulb-like structure determined for the oxidized as well as reduced micelle

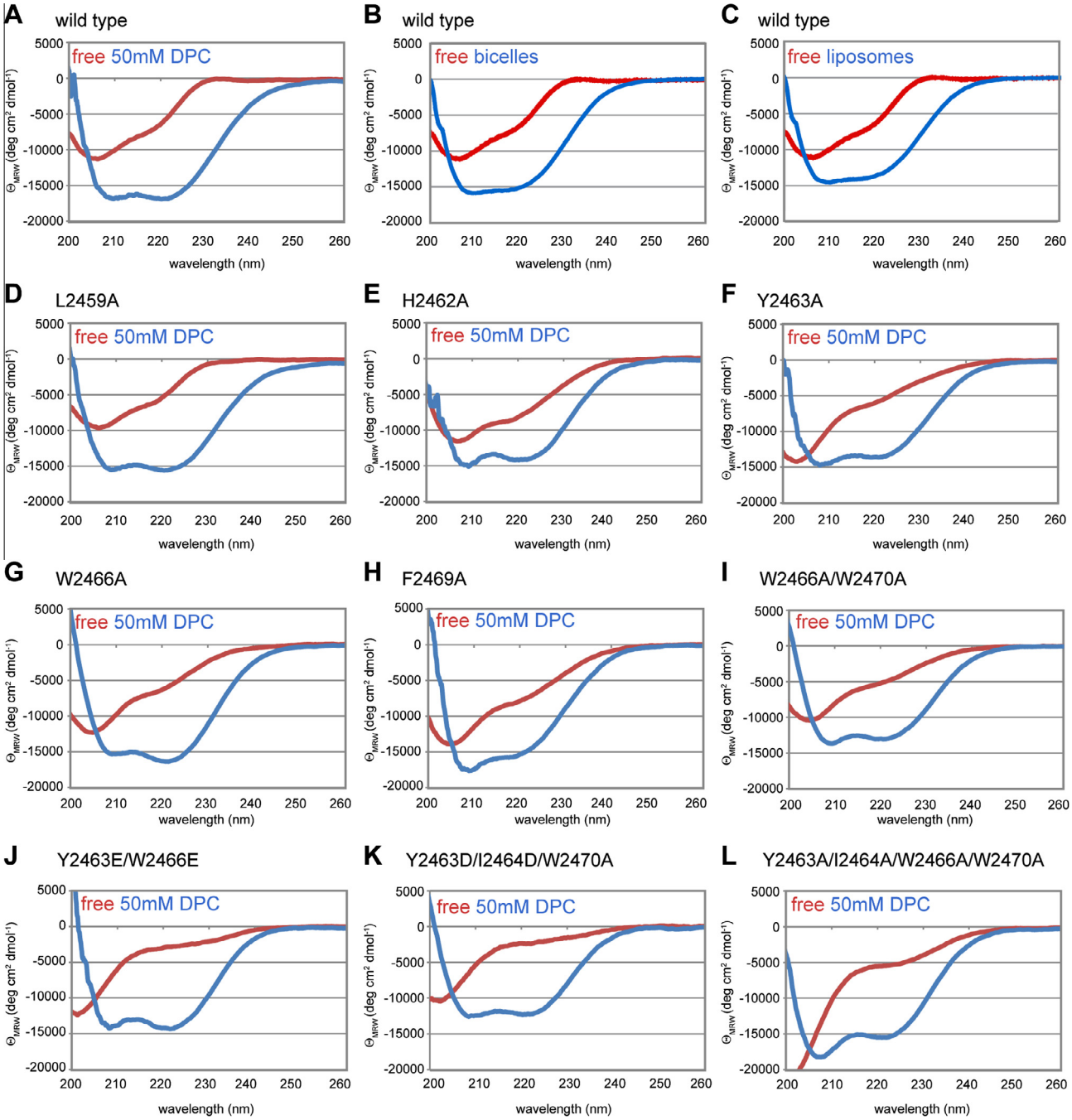

Fig. 5. CD spectra of the untagged yeast TOR1 FATC domain and mutants in the absence (red) and presence of membrane mimetics (blue). (A–C) CD spectra of wild type y1fatc in the absence and presence of DPC micelles (always 50 mM DPC), DMPC/DihePC bicelles and DMPC SUVs. The CD spectra of bicelles are generally of lower quality since the bicelles produce themselves a very strong CD signal (see SI Fig. S6A). (D–L) CD spectra of mutants that were prepared in the untagged form. The respective mutations are indicated at the top of each plot. The determination of the concentration for the quadruple alanine mutant (L) based on UV measurements was not as accurate as for the other mutants since this mutant had only one phenylalanine left and thus a very low extinction coefficient. The color coding of the spectra is given in each plot. SI Fig. S6 shows additionally the CD spectra of bicelles and SUVs in buffer and in the presence of untagged y1fatc-Y2463D/I2464D/W2466A and GB1-tagged y1fatc-L2459A.

immersed state (Fig. 1A and [23]). However, also these three mutants were still able to interact with membrane mimetic DPC micelles (Fig. 2F, SI Fig. S3C,D). Moreover, based on the spectral differences after the addition of the reducing agent TCEP to two of them (SI Fig. S3E–F), they were still able to form the disulfide bond. This was presumably possible because G2465 was replaced by the still relatively small serine and because one or more residues with bulky side chain such as W2466 had additionally been replaced by smaller residues. In summary, all tested new 13 as well as the earlier generated W2466A and W2466A/W2470 y1fatc mutants could still interact with DPC micelles at the typically used rather high concentrations ($\geqslant$50 mM, Table 1 and [23]).

3.3. Mutation of up to 6 residues of y1fatc membrane anchor did not abrogate the interaction with DihepPC/DMPC bicelles

Because DPC micelles are rather small spherical particles with a high curvature and because DPC is also used as detergent, we further analyzed the association of various y1fatc mutants with DMPC/DihepPC bicelles that have a planar region consisting of a

lipid bilayer (Fig. 3A, SI Fig. S1B). The superpositions of the ^{1}H-^{15}N-HSQC spectra of wild type and several mutant y1fatc proteins in the free form and with DMPC/DihepPC bicelles are shown in Fig. 3 (A–B untagged wild type and Y2463D/I2464D/W2466A, C–F Gb1-tagged y1fatc-L2459A, -Y2463A, -Y2463E/W2466E, -H2462R/Y2463D/I2464D/G2465S/W2466S/F2469D) and SI Fig. S4 (Gb1-tagged y1fatc-Y2463D/I2464D/W2466E/W2470R, -H2462R/Y2463D/I2464D/W2466A/F2469D, -G2465S/W2466S). Indicated by the strong spectral differences between the spectra in the absence (in black) and presence of bicelles (in red), all tested y1fatc mutants (Table 1) showed still a significant affinity for bicelles at the used high lipid concentrations (~200–240 mM), even y1fatc-H2462R/Y2463D/I2464D/G2465S/W2466S/F2469D (Fig. 3F) in which 6 residues of the membrane anchor had been replaced by polar or charged residues.

3.4. Mutation of only a single residue of the y1fatc membrane anchor could significantly reduce the affinity for DMPC liposomes

The observation that all tested y1fatc mutants could still interact with DPC micelles or DihepPC/DMPC bicelles at the usually used high concentrations, suggested that these two membrane mimetics may not be ideally suited to detect significant binding differences that allow to find a mutation that may abrogate the interaction of full-length TOR with cellular membranes in *in vivo* experiments. Therefore, we finally analyzed the interaction of several y1fatc mutants with DMPC SUVs that may better mimic natural membranes (Fig. 4A, SI Fig. S1B) and that are usually prepared from lower lipid concentrations (final concentration in sample <30 mM DMPC). As described above untagged oxidized wild type y1fatc interacts with DMPC liposomes of the SUV type, resulting in the disappearance of the majority of its resonances (Fig. 1B). The same can be observed if DMPC SUVs are added to GB1-tagged wild type y1fatc (Fig. 4A). If L2459 in the N-terminal part of the membrane anchor (Fig. 1A) was replaced by the smaller but still hydrophobic alanine, y1fatc could still interact with DMPC SUVs (Fig. 4B). However, replacement of only one or two aromatic residues in the more central region of the membrane anchor (Fig. 1A) by alanine or glutamate (Y2463A & Y2463E/W2466E Fig. 4C–D, W2466A & W2466A/W2470A SI Fig. S5C–D) in GB1-tagged or untagged y1fatc basically abrogated the interaction with DMPC SUVs. Accordingly the ^{1}H-^{15}N-HSQC spectra in the presence of liposomes, which are shown in red, almost completely superimpose with ones in the absence of liposomes in black, which are thus mostly not visible anymore. Not astonishingly, mutation of three or more residues resulted also not in significant spectral changes (SI Fig. S5B, F–K, Table 1).

Since SUVs at the usually used low concentrations allowed to clearly detect binding differences between y1fatc wild type and mutant proteins, we finally analyzed if a comparison of the titrations with DPC at lower concentrations (0 to $\leqslant$30 mM) provides complementary insights. Fig. 4E and F shows the titrations of the GB1-tagged y1fatc Y2463A and Y2463E/W2466E with DPC. Both mutants did not show significant spectral changes with liposomes (Fig. 4C and D). In the titration with DPC, the majority of peaks for the single mutant Y2463A (Fig. 4E) disappear already at the first concentration step (2.5 mM) above the CMC of DPC (1.1 mM). Thus this mutant behaved in the titration similar as the wild type and the W2466A and W2466A/W2470A mutants [23]. In contrast, the double mutant Y2463E/W2466E (Fig. 4F) showed still most peaks at 2.5 mM DPC and the majority of signals started only to disappear or shift at the next titration step (5 mM DPC). Therefore the relative affinity for DPC micelles is clearly lower for the Y2463E/W2466E compared to the Y2463A mutant. Note that the peaks for the micelle immersed state become usually only well visible at higher DPC concentrations when the equilibrium is further shifted to the bound state (see for example the spectra of the Y2463A and Y2463E/W2466E mutants in the presence of 100 mM DPC in Fig. 2B and C).

In summary, the NMR-monitored interaction studies of y1fatc with different membrane mimetics at different concentrations showed that at least in case of the TOR FATC domain high concentrations of micelles and bicelles appear not suitable to find rather moderate mutations that abrogate membrane interactions. Only the use of DMPC SUVs at low concentrations resulted in clearly detectable binding differences between wild type and different mutant y1fatc proteins. Complementary titrations with low concentrations of DPC allowed further to qualitatively compare the relative affinities for DPC micelles.

3.5. CD data indicated that the presence of membrane mimetic micelles, bicelles, and liposomes increase the content of α-helical secondary structure. The tested single to quadruple mutants showed the same effect with micelles

Since only the structures of the oxidized and reduced wild type DPC micelle immersed states have been determined previously [23], we first analyzed by CD, if the presence of bicelles and SUVs results also in an increase of the α-helical secondary structure content. As can be seen from a comparison of Fig. 5A–C this is indeed the case. The CD data in presence of bicelles is usually of significantly less quality since bicelles themselves produce already a huge signal (SI Fig. S6A). The signal from SUVs at the usually used low concentrations is generally rather small (SI Fig. S6B), however can produce a positive signal of a few mdeg (SI of [34]). For both bicelles and SUVs the produced signal can slightly vary from one preparation to another, especially if the lipid concentration is not exactly the same. For this reason the buffer reference measurements should always be done using the same batch of bicelle or SUV preparation as used for the protein sample (see also SI of [34]). Since DPC micelles produce no significant signal (SI of [34]) they are overall more convenient to be used for CD measurements.

Based on the CD measurements of wild type y1fatc (Fig. 4A) and 9 different mutants with one to four mutations, addition of DPC micelles (50 mM, Fig. 4D–L) resulted for all in a significant increase in the α-helical secondary structure content. This is consistent with the ability to interact with DPC micelles indicated by the NMR data (Fig. 2, SI Figs. S2 and S3). However, the ratio of the CD signal at the α-helix typical minima at 208 and 222 nm varied slightly. Whereas the spectra of the free y1fatc mutants L2459A and H2462A have overall a similar shape as the wild type, indicating a similar degree of α-helicity in the free state, the spectra of the y1fatc mutants Y2463A, W2466A, F2469A, W2466A/W2470A, Y2463E/W2466E, Y2463D/I2464D/W2470A, and the quadruple alanine mutant Y2463A/I2464A/W2466A/W2470A appeared to have to a varying degree a bigger contribution from an unfolded protein signal, which was the most pronounced for the quadruple mutant. The CD spectra of the quadruple alanine mutant and the F2469A mutant indicate also a slightly higher contribution from an unfolded protein signal in DPC micelle immersed state. For the untagged triple y1fatc mutant Y2463D/I2464D/W2466A and the GB1-tagged single mutant L2459A we also recorded CD spectra in the absence and presence of bicelles and SUVs (SI Fig. S6C–F). Consistent with the NMR data that indicated an interaction with bicelles but no significant one with SUVs for the Y2463D/I2464D/W2466A mutant (Fig. 3B, SI Fig. S5B), bicelles resulted in an increase of α-helical secondary structure, whereas the SUVs induced no significant CD spectral changes. Also in agreement with the NMR data (Figs. 3C and 4B), the moderate L2459 mutant showed CD spectral changes with both membrane mimetics. Thus the CD-monitored interaction data overall confirmed the NMR-monitored one.

4. Discussion

The membrane anchor in the FATC domain may represent one component of a network of protein–lipid/–membrane and protein–protein interactions mediating and regulating TOR localization, thus allowing a specific local signaling response. To better understand the role of different residues of the FATC membrane anchor for peripheral membrane association and to establish a methodological framework to do this, we analyzed the interactions of a whole ensemble of mutants with different membrane mimetics by NMR and CD spectroscopy (Table 1, Figs. 2–5, SI Figs. S2–S6). All mutants, even ones in which up to 6 or 7 residues of the hydrophobic C-terminal region had been mutagenized to mostly charged residues, could still interact with DPC micelles and DihepPC/DMPC bicelles (Figs. 2 and 3, SI Figs. S2–S4) at the usually used rather high concentrations. An abrogation of y1fatc-membrane mimetic interactions could only be detected if SUVs composed of DMPC were used at low concentrations (Fig. 4A–D, SI Fig. S5). In this experimental set-up, even mutation of only one hydrophobic residue in the center of the C-terminal loop had a clearly detectable effect. The different association behavior of the y1fatc mutants with micelles and bicelles compared to liposomes can be explained twofold. First, using micelles or bicelles the total concentration of the used detergents or lipids is rather high and consequently also the available membrane mimetic surface area. The used DPC concentrations were in the range of 50–200 mM and the total lipid concentrations in the bicelle sample was ~200–240 mM. In contrast, the total lipid concentration in the SUV preparation in the present samples was significantly below 30 mM since pure DMPC cannot easily be resuspended at high concentrations and in addition some of the lipid is lost when separating the small from larger uni- and multilamellar vesicles by centrifugation. The latter results in a disadvantage of this SUV preparation method, namely that the final lipid concentration after centrifugation may vary from one preparation to another depending on different factors (storage time of lipids before use, exact ultrasonication time and temperature, etc.). This hampers a quantitative comparison of the respective binding data. In 1D ^{1}H NMR spectra, one does due to the large size of SUVs only see small lipid signals and not as for DPC micelles or DMPC/DihepPC bicelles really large ones, which allow to easily compare the lipid content in the samples containing the latter two membrane mimetics. Besides established methods such as dynamic light scattering, the CD signal may be used to compare different liposome preparations using the described as well as other methods. The example CD spectrum in SI Fig. S6 shows only a weak positive signal, however depending on the used concentration and the preparation, SUVs can show a CD signal of several mdeg around 215 nm [34]. For future similar binding studies, more uniform SUV preparations may be obtained by using an extruder with a defined pore size. A second reason for the different binding behavior of y1fatc to micelles and bicelles versus SUVs may further be a somewhat higher affinity of the TOR FATC membrane anchor for curved and/or less densely packed membrane surfaces. This would be in agreement with the observation that some of the tested mutants can interact with rather low concentrations of DPC (around 1.1–5 mM, Fig. 4E and F and [23]). DPC micelles are rather small, spherical particles (Fig. 2A, SI Fig. S1B) that contain ~50–60 DPC molecules, resulting in a molecular weight of ~19 kDa [47]. Bicelles have a rather planar bilayer region that is formed by a long chain phospholipid such as DMPC (Fig. 3A, SI Fig. S1B). However the rim that is formed by a short chain lipid such as DihepPC shows as micelles also a high curvature. The molecular weight of bicelles is usually >250 kDa [48]. Even liposomes of the SUV type are much larger than bicelles. Although they are as micelles approximately spherical, they are less curved since the radius is much larger (Fig. 4A, SI Fig. S1B). Overall, our binding studies with different mutants suggest that for proteins with a rather high and broad affinity for different membrane mimetics, SUVs that are usually used at lower concentrations appear generally better suited to detect binding differences and thus to find mutants that may also abrogate membrane association in localization studies in cells. In addition, complementary titrations with DPC at low concentrations (0 to ~30 mM) such as shown in Fig. 4E and F can be used to compare the relative membrane mimetic binding affinity of different mutants. These studies show however also that every membrane mimetic has its advantages and disadvantages and that it is overall not a trivial task to choose the right concentration to mimic the available membrane surface area in the cell, also because the latter is experimentally not easily determined. Nevertheless, testing in cellular localization and functional assays different TOR full-length proteins containing FATC mutations, which abrogated the interaction with SUVs in the presented data (Table 1, see also detailed discussion below), should provide useful insights about the role of the FATC domain for TOR localization and function.

The observation that mutants of the TOR FATC domain with as many as 6–7 replacements could still interact with DPC micelles and DihepPC/DMPC bicelles suggest two things (Table 1). First, hydrophobic interactions of the remaining hydrophobic residues in the membrane anchor (e.g. W2470, P2468, L2459, and I2456 in the mutant y1fatc H2462R/Y2463D/I2464D/G2465S/W2466S/F2469D) as well as additional polar interactions of the introduced charged residues with the positive and negative charges of the choline headgroup are still sufficient to maintain a well detectable affinity for micelles and bicelles. Moreover, the interactions with residues N-terminal of the hydrophobic bulb like regions may be more important for the interactions with membrane mimetics than initially expected. Second, the observation that a rather highly mutated FATC domain showed still significant spectral changes with micelles or bicelles may suggest that many peptides or small proteins may unspecifically interact with these membrane mimetics. However, we have ourselves analyzed several small proteins or peptides that do not interact with DPC micelles and/or DihepPC/DMPC bicelles. The NMR data from the present (Figs. 2–4, SI Figs. S3–S5) as well as from previous studies indicated that the B1 domain of streptococcal protein G (GB1), alone or fused to other proteins, does not interact with DPC micelles, DihepPC/DMPC bicelles, or SUVs [24,39]. Recently, we further characterized the interaction of the N-terminal domain of Formin C, of a 26-mer peptide corresponding to a large unstructured loop of this domain, and of a mutant form lacking this loop with different membrane mimetics. To mimic the restriction of mobility in the full-length protein, the 26-mer peptide could further be circularized by oxidation of terminal cysteines. Whereas the full N-terminal domain and the mutant form lacking the loop showed strong spectral changes in the presence of pure DPC micelles and even more if containing negatively charged lipids, neither the reduced nor the oxidized 26-mer peptide showed any spectral changes in CD or NMR spectra upon addition of 50 mM DPC [49]. In contrast to the y1fatc protein analyzed in this study, the Formin C N-terminal domain showed only very minor spectral changes with bicelles, presumably because its interaction with membrane mimetics may be more sensitive to the packing and accessibility of the hydrophobic acyl chains and not only to the curvature [49]. Another example for a protein region that shows no interactions with DPC micelles is the N-terminal natively unstructured region of the mycobacterial kinase G (PknG, residues 1–76, Uniprot ID P65728) (unpublished data). Finally, two more examples for proteins that show as all tested TOR FATC mutants strong spectral changes with micelles and bicelles but only weak ones with SUVs are the FRB domain of TOR [34] and the FATC domain of the PIKK DNA-PKcs [24]. Generally, the different affinities for different membrane mimetics can often be rationalized based on the current knowledge of the protein

function. Proteins that are expected to bind only temporarily to very specific membrane regions, show overall only a significant affinity for membrane mimetics that mimic features of the natural target membranes such as the presence of specific lipids like PIPs or the surface curvature [44,50–52].

The interaction studies with SUVs indicated that replacement of one or two residues may be sufficient to also abrogate the binding of the TOR FATC domain to cellular membranes. Based on our data the moderate single mutations Y2463A (Fig. 4C) and W2466A (SI Fig. S5C) and, or the more harsh double mutants Y2463E/W2466E (Fig. 4D) W2466A/W270A (SI Fig. S5D) could be useful to be incorporated in full-length yeast TOR1 or TOR from a higher eukaryote for *in vivo* studies to evaluate the role of the FATC domain for the localization and function of TOR. All three residues are in the bulb-like C-terminal region (Fig. 1A). Based on the structures of the free oxidized and the micelle immersed oxidized and reduced states Y2463 and W2466 appear not to be too critical for loop formation but rather for its interactions, whereas W2470 mediates some intramolecular contacts [18,23]. The comparison of the ^{1}H-^{15}N-HSQC spectra of all these mutants with the one of the wild type indicate that they all can form the disulfide bond between C2460 and C2467 (Figs. 2–4 and [23]). Indicated by the deeper minimum around 222 nm in the CD data (Fig. 5), the alanine mutants W2466A, W2466A/W2470A, and Y2463A maintain in the free state a slightly higher degree of α-helicity as the double glutamate mutant Y2463E/W2466E. Based on the alignment of the sequences of the FATC domain of different human PIKKs (SI Fig. S1A), mutation of these positions is also interesting with respect to the other PIKKs. The position corresponding to W2466 in y1fatc is in all PIKKs occupied by a tryptophan. The position corresponding to Y2463 is in all except TRRAP occupied by an aromatic residue. TRRAP differs overall a bit from the consensus features of the other PIKKs, also since it is the only family member not showing catalytic kinase activity [13]. The position corresponding to y1fatc W2470 is in all occupied by a hydrophobic residue. If the effect of mutating only one or two residues may not be sufficient to abrogate the interaction with cellular membranes, because the interaction of the large membrane mimetic interface of y1fatc is stronger than with low concentrations of SUVs, the tested triple or quadruple mutants (Table 1) may be introduced in full-length TOR for *in vivo* studies.

Based on a docking model of a newly determined crystal structure of truncated human TOR in complex with LST8 with a substrate peptide, the FATC domain interacts with the kinase domain and with one residue also with LST8, providing a hydrophobic surface region that may not only mediate substrate [53], but also membrane interactions. Y2452 and W2545, corresponding to Y2463 and W2466 in y1fatc, are part of this hydrophobic patch. Thus mutating either one or both of these residues may influence substrate binding as well as interactions with membranes and regulator proteins, some of which are known to reside at membranes such as farnesylated Rheb [54] or the Ragulator-Rag complex [28]. Therefore, future *in vivo* localization studies have to include reference experiments such as in vitro kinase or interaction assays to separate the different effects. In addition it has to be considered that the interaction of the FATC domain with the kinase domain or other components of the two TOR complexes as well as with membrane lipids and regulator proteins may be modified by cellular redox agents [18,23]. Additional information about the accessibility of the FATC domain can be obtained from EM structures of yeast TOR1 alone and in complex with the Raptor yeast-homolog KOG1. In the uncomplexed form, the FATC domain appeared like a protruding finger and thus accessible for potential membrane interactions. Due to the low resolution (~25 Å) the accessibility in the complexed form could however not be clearly evaluated [55].

In conclusion, we analyzed in detail the effect of mutating one or more residue of the hydrophobic membrane anchor of the FATC domain of TOR on the association behavior with membrane mimetic micelles, bicelles, and liposomes. For a protein like y1fatc, with a broad membrane mimetic binding affinity, only NMR-based interaction studies employing SUVs at low concentrations were useful to clearly detect mutations that may also abrogate membrane interactions *in vivo*. Complementary titration studies with DPC at low concentrations allowed additionally to compare differences in the binding affinity for mutants showing a significantly reduced interaction with liposomes. The complementary CD data confirmed the NMR interaction data and allowed to estimate the differences in the secondary structure content between the free and micelle immersed wild type and mutant proteins. Some of the mutants not binding to liposomes may be incorporated in full-length TOR for *in vivo* functional and localization studies, which will help to better understand the role of the redox-sensitive FATC domain for the regulation of TOR localization at different cellular membranes and its local signaling activity. Recent studies suggest that the ability to interact with membrane mimetics is also shared by the FATC domains of the other PIKKs [24]. The presented binding data of different TOR FATC mutants it also helpful to better rationalize, why the FATC domains of all tested PIKKs can interact with membrane mimetics, although with apparently somehow different preferences for different membrane properties such as surface charge, shape, and curvature and the acyl chain packing density. Finally, the small FATC domain might be linked to other proteins or substances to tether them to membrane mimetics, for example lipid bilayers attached to solid phases.

Funding sources

This work was supported by Grants from the German Research Foundation to S.A.D. (DA 1195/3-1 and collaborative research center 1035, subproject B04). S.A.D and L.A.M.S. acknowledge further financial support from the TUM diversity and talent management office and S.A.D. additionally from the project 'metabolic dysfunction' of the Helmholtz Zentrum München.

Acknowledgements

The following (former) TUM biochemistry bachelor students we thank for their contributions to some of the protein purifications and/or some of the NMR- and CD-measurements: Melanie Meier, Ann-Kathrin Flörsheimer, Tanja Kraus, Tamara Heermann. The groups of Prof. Dr. S. Grzesiek and Prof. Dr. M. Hall from the Biozentrum in Basel we acknowledge for support during the initial phase of the project around TOR. Prof. Dr. M. Sattler from the TU München/Helmholtz Zentrum München I thank very much for hosting my group and for his continuous support.

Appendix A. Supplementary data

Supplementary data associated with this article can be found, in the online version, at http://dx.doi.org/10.1016/j.febslet.2014.03.031.

References

[1] Laplante, M. and Sabatini, D.M. (2012) MTOR signaling in growth control and disease. Cell 149, 274–293.
[2] Dazert, E. and Hall, M.N. (2011) MTOR signaling in disease. Curr. Opin. Cell Biol. 23, 744–755.
[3] Yang, Z. and Ming, X.F. (2012) MTOR signalling: the molecular interface connecting metabolic stress, aging and cardiovascular diseases. Obes. Rev. 13 (Suppl 2), 58–68.

[4] Blagosklonny, M.V. and Hall, M.N. (2009) Growth and aging: a common molecular mechanism. Aging (Albany, NY) 1, 357–362.
[5] Appenzeller-Herzog, C. and Hall, M.N. (2012) Bidirectional crosstalk between endoplasmic reticulum stress and mTOR signaling. Trends Cell Biol. 22, 274–282.
[6] Loewith, R., Jacinto, E., Wullschleger, S., Lorberg, A., Crespo, J.L., Bonenfant, D., Oppliger, W., Jenoe, P. and Hall, M.N. (2002) Two TOR complexes, only one of which is rapamycin sensitive, have distinct roles in cell growth control. Mol. Cell 10, 457–468.
[7] Sarbassov, D.D., Ali, S.M., Sengupta, S., Sheen, J.H., Hsu, P.P., Bagley, A.F., Markhard, A.L. and Sabatini, D.M. (2006) Prolonged rapamycin treatment inhibits mTORC2 assembly and Akt/PKB. Mol. Cell 22, 159–168.
[8] Bosotti, R., Isacchi, A. and Sonnhammer, E.L. (2000) FAT: a novel domain in PIK-related kinases. Trends Biochem. Sci. 25, 225–227.
[9] Knutson, B.A. (2010) Insights into the domain and repeat architecture of target of rapamycin. J. Struct. Biol. 170, 354–363.
[10] Groves, M.R. and Barford, D. (1999) Topological characteristics of helical repeat proteins. Curr. Opin. Struct. Biol. 9, 383–389.
[11] Choi, J., Chen, J., Schreiber, S.L. and Clardy, J. (1996) Structure of the FKBP12-rapamycin complex interacting with the binding domain of human FRAP. Science 273, 239–242.
[12] Takahashi, T., Hara, K., Inoue, H., Kawa, Y., Tokunaga, C., Hidayat, S., Yoshino, K., Kuroda, Y. and Yonezawa, K. (2000) Carboxyl-terminal region conserved among phosphoinositide-kinase-related kinases is indispensable for mTOR function in vivo and in vitro. Genes Cells 5, 765–775.
[13] Lempiainen, H. and Halazonetis, T.D. (2009) Emerging common themes in regulation of PIKKs and PI3Ks. EMBO J. 28, 3067–3073.
[14] Morita, T., Yamashita, A., Kashima, I., Ogata, K., Ishiura, S. and Ohno, S. (2007) Distant N- and C-terminal domains are required for intrinsic kinase activity of SMG-1, a critical component of nonsense-mediated mRNA decay. J. Biol. Chem. 282, 7799–7808.
[15] Hoke, S.M., Irina Mutiu, A., Genereaux, J., Kvas, S., Buck, M., Yu, M., Gloor, G.B. and Brandl, C.J. (2010) Mutational analysis of the C-terminal FATC domain of *Saccharomyces cerevisiae* Tra1. Curr. Genet. 56, 447–465.
[16] Jiang, X., Sun, Y., Chen, S., Roy, K. and Price, B.D. (2006) The FATC domains of PIKK proteins are functionally equivalent and participate in the Tip60-dependent activation of DNA-PKcs and ATM. J. Biol. Chem. 281, 15741–15746.
[17] Mordes, D.A., Glick, G.G., Zhao, R. and Cortez, D. (2008) TopBP1 activates ATR through ATRIP and a PIKK regulatory domain. Genes Dev. 22, 1478–1489.
[18] Dames, S.A., Mulet, J.M., Rathgeb-Szabo, K., Hall, M.N. and Grzesiek, S. (2005) The solution structure of the FATC domain of the protein kinase target of rapamycin suggests a role for redox-dependent structural and cellular stability. J. Biol. Chem. 280, 20558–20564.
[19] Sarbassov, D.D. and Sabatini, D.M. (2005) Redox regulation of the nutrient-sensitive raptor-mTOR pathway and complex. J. Biol. Chem. 280, 39505–39509.
[20] Yoshida, S., Hong, S., Suzuki, T., Nada, S., Mannan, A.M., Wang, J., Okada, M., Guan, K.L. and Inoki, K. (2011) Redox regulates mammalian target of rapamycin complex 1 (mTORC1) activity by modulating the TSC1/TSC2-Rheb GTPase pathway. J. Biol. Chem. 286, 32651–32660.
[21] Neklesa, T.K. and Davis, R.W. (2008) Superoxide anions regulate TORC1 and its ability to bind Fpr1:rapamycin complex. Proc. Natl. Acad. Sci. USA 105, 15166–15171.
[22] Zhang, J., Kim, J., Alexander, A., Cai, S., Tripathi, D.N., Dere, R., Tee, A.R., Tait-Mulder, J., Di Nardo, A., Han, J.M., Kwiatkowski, E., Dunlop, E.A., Dodd, K.M., Folkerth, R.D., Faust, P.L., Kastan, M.B., Sahin, M. and Walker, C.L. (2013) A tuberous sclerosis complex signalling node at the peroxisome regulates mTORC1 and autophagy in response to ROS. Nat. Cell Biol. 15, 1186–1196.
[23] Dames, S.A. (2010) Structural basis for the association of the redox-sensitive target of rapamycin FATC domain with membrane-mimetic micelles. J. Biol. Chem. 285, 7766–7775.
[24] Sommer, L.A., Schaad, M. and Dames, S.A. (2013) NMR- and circular dichroism-monitored lipid binding studies suggest a general role for the FATC domain as membrane anchor of phosphatidylinositol 3-kinase-related kinases (PIKK). J. Biol. Chem. 288, 20046–20063.
[25] Berchtold, D. and Walther, T.C. (2009) TORC2 plasma membrane localization is essential for cell viability and restricted to a distinct domain. Mol. Biol. Cell 20, 1565–1575.
[26] Drenan, R.M., Liu, X., Bertram, P.G. and Zheng, X.F. (2004) FKBP12-rapamycin-associated protein or mammalian target of rapamycin (FRAP/mTOR) localization in the endoplasmic reticulum and the Golgi apparatus. J. Biol. Chem. 279, 772–778.
[27] Kunz, J., Schneider, U., Howald, I., Schmidt, A. and Hall, M.N. (2000) HEAT repeats mediate plasma membrane localization of Tor2p in yeast. J. Biol. Chem. 275, 37011–37020.
[28] Sancak, Y., Bar-Peled, L., Zoncu, R., Markhard, A.L., Nada, S. and Sabatini, D.M. (2010) Ragulator-Rag complex targets mTORC1 to the lysosomal surface and is necessary for its activation by amino acids. Cell 141, 290–303.
[29] Wedaman, K.P., Reinke, A., Anderson, S., Yates 3rd, J., McCaffery, J.M. and Powers, T. (2003) Tor kinases are in distinct membrane-associated protein complexes in *Saccharomyces cerevisiae*. Mol. Biol. Cell 14, 1204–1220.
[30] Partovian, C., Ju, R., Zhuang, Z.W., Martin, K.A. and Simons, M. (2008) Syndecan-4 regulates subcellular localization of mTOR Complex2 and Akt activation in a PKCalpha-dependent manner in endothelial cells. Mol. Cell 32, 140–149.
[31] Liu, X. and Zheng, X.F. (2007) Endoplasmic reticulum and Golgi localization sequences for mammalian target of rapamycin. Mol. Biol. Cell 18, 1073–1082.
[32] Zhang, X., Shu, L., Hosoi, H., Murti, K.G. and Houghton, P.J. (2002) Predominant nuclear localization of mammalian target of rapamycin in normal and malignant cells in culture. J. Biol. Chem. 277, 28127–28134.
[33] Zinzalla, V., Stracka, D., Oppliger, W. and Hall, M.N. (2011) Activation of mTORC2 by association with the ribosome. Cell 144, 757–768.
[34] Rodriguez Camargo, D.C., Link, N.M. and Dames, S.A. (2012) The FKBP-rapamycin binding domain of human TOR undergoes strong conformational changes in the presence of membrane mimetics with and without the regulator phosphatidic acid. Biochemistry 51, 4909–4921.
[35] Fang, Y., Vilella-Bach, M., Bachmann, R., Flanigan, A. and Chen, J. (2001) Phosphatidic acid-mediated mitogenic activation of mTOR signaling. Science 294, 1942–1945.
[36] Mugler, A., Bailey, A.G., Takahashi, K. and Ten Wolde, P.R. (2012) Membrane clustering and the role of rebinding in biochemical signaling. Biophys. J. 102, 1069–1078.
[37] Mugler, A., Tostevin, F. and Ten Wolde, P.R. (2013) Spatial partitioning improves the reliability of biochemical signaling. Proc. Natl. Acad. Sci. USA.
[38] Koenig, B.W., Rogowski, M. and Louis, J.M. (2003) A rapid method to attain isotope labeled small soluble peptides for NMR studies. J. Biomol. NMR 26, 193–202.
[39] Sommer, L.A.M., Meier, M.A. and Dames, S.A. (2012) A fast and simple method for probing the interaction of peptides and proteins with lipids and membrane-mimetics using GB1 fusion proteins and NMR spectroscopy. Protein Sci. 21, 1566–1570.
[40] Delaglio, F., Grzesiek, S., Vuister, G.W., Zhu, G., Pfeifer, J. and Bax, A. (1995) NMRPipe: a multidimensional spectral processing system based on UNIX pipes. J. Biomol. NMR 6, 277–293.
[41] Johnson, B.A. (2004) Using NMRView to visualize and analyze the NMR spectra of macromolecules. Methods Mol. Biol. 278, 313–352.
[42] Liu, W. and Caffrey, M. (2006) Interactions of tryptophan, tryptophan peptides, and tryptophan alkyl esters at curved membrane interfaces. Biochemistry 45, 11713–11726.
[43] Sun, H., Greathouse, D.V., Andersen, O.S. and Koeppe 2nd, R.E. (2008) The preference of tryptophan for membrane interfaces: insights from N-methylation of tryptophans in gramicidin channels. J. Biol. Chem. 283, 22233–22243.
[44] Kutateladze, T.G., Capelluto, D.G., Ferguson, C.G., Cheever, M.L., Kutateladze, A.G., Prestwich, G.D. and Overduin, M. (2004) Multivalent mechanism of membrane insertion by the FYVE domain. J. Biol. Chem. 279, 3050–3057.
[45] Ahn, H.C., Juranic, N., Macura, S. and Markley, J.L. (2006) Three-dimensional structure of the water-insoluble protein crambin in dodecylphosphocholine micelles and its minimal solvent-exposed surface. J. Am. Chem. Soc. 128, 4398–4404.
[46] Nanga, R.P., Brender, J.R., Xu, J., Hartman, K., Subramanian, V. and Ramamoorthy, A. (2009) Three-dimensional structure and orientation of rat islet amyloid polypeptide protein in a membrane environment by solution NMR spectroscopy. J. Am. Chem. Soc. 131, 8252–8261.
[47] Tieleman, D.P., van der Spoel, D. and Berendsen, H.J.C. (2000) Molecular dynamics simulations of dodecylphosphocholine micelles at three different aggregate sizes: micellar structure and chain relaxation. J. Phys. Chem. B 104, 6380–6388.
[48] Whiles, J.A., Deems, R., Vold, R.R. and Dennis, E.A. (2002) Bicelles in structure-function studies of membrane-associated proteins. Bioorg. Chem. 30, 431–442.
[49] Dames, S.A., Junemann, A., Sass, H.J., Schonichen, A., Stopschinski, B.E., Grzesiek, S., Faix, J. and Geyer, M. (2011) Structure, dynamics, lipid binding, and physiological relevance of the putative GTPase-binding domain of *Dictyostelium formin* C. J. Biol. Chem. 286, 36907–36920.
[50] Serth, J., Lautwein, A., Frech, M., Wittinghofer, A. and Pingoud, A. (1991) The inhibition of the GTPase activating protein-Ha-ras interaction by acidic lipids is due to physical association of the C-terminal domain of the GTPase activating protein with micellar structures. EMBO J. 10, 1325–1330.
[51] Ramalingam, N., Zhao, H., Breitsprecher, D., Lappalainen, P., Faix, J. and Schleicher, M. (2010) Phospholipids regulate localization and activity of mDia1 formin. Eur. J. Cell Biol. 89, 723–732.
[52] Zimmerberg, J. and Kozlov, M.M. (2006) How proteins produce cellular membrane curvature. Nat. Rev. Mol. Cell Biol. 7, 9–19.
[53] Yang, H., Rudge, D.G., Koos, J.D., Vaidialingam, B., Yang, H.J. and Pavletich, N.P. (2013) MTOR kinase structure, mechanism and regulation. Nature 497, 217–223.
[54] Buerger, C., DeVries, B. and Stambolic, V. (2006) Localization of Rheb to the endomembrane is critical for its signaling function. Biochem. Biophys. Res. Commun. 344, 869–880.
[55] Adami, A., Garcia-Alvarez, B., Arias-Palomo, E., Barford, D. and Llorca, O. (2007) Structure of TOR and its complex with KOG1. Mol. Cell 27, 509–516.